

# Three-Temperature Modeling of Carrier-Phonon Interactions in Thin GaAs Film Structures Irradiated by Picosecond Pulse Lasers

**Seong Hyuk Lee\***

*School of Mechanical Engineering, Chung-Ang University,  
221 Heuksuk-dong, Dongjak-gu, Seoul 156-756, Korea*

**Junghee Lee**

*School of Mechanical Engineering, Chung-Ang University,  
Seoul 156-756, Korea*

**Kwan-Gu Kang**

*Micro Thermal System Research Center, Seoul National University,  
Seoul 151-742, Korea*

**Joon Sik Lee**

*School of Mechanical and Aerospace Engineering, Seoul National University,  
Seoul 151-742, Korea*

This article investigates numerically the carrier-phonon interactions in thin gallium arsenide (GaAs) film structures irradiated by subpicosecond laser pulses to figure out the role of several recombination processes on the energy transport during laser pulses and to examine the effects of laser fluences and pulses on non-equilibrium energy transfer characteristics in thin film structures. The self-consistent hydrodynamic equations derived from the Boltzmann transport equations are established for carriers and two different types of phonons, i.e., acoustic phonons and longitudinal optical (LO) phonons. From the results, it is found that the two-peak structure of carrier temperatures depends mainly on the pulse durations, laser fluences, and nonradiative recombination processes, two different phonons are in nonequilibrium state within such lagging times, and this lagging effect can be neglected for longer pulses. Finally, at the initial stage of laser irradiation, SRH recombination rates increases sufficiently because the abrupt increase in carrier number density no longer permits Auger recombination to be activated. For thin GaAs film structures, it is thus seen that Auger recombination is negligible even at high temperature during laser irradiation.

**Key Words :** Ultra-Short Pulse Lasers, Gallium Arsenide, Optical Phonons, Acoustic Phonons, Carriers, Nonequilibrium, SRH (Shockely-Read-Hall), Auger Recombination

## Nomenclature

$C$  : Heat capacity per unit volume,  $J/m^3 K$

$E_g$ : Band gap, eV

---

\* Corresponding Author,

**E-mail :** shlee89@cau.ac.kr

**TEL :** +82-2-820-5254; **FAX :** +82-2-814-9476

School of Mechanical Engineering, Chung-Ang University, 221 Heuksuk-dong, Dongjak-gu, Seoul 156-756, Korea. (Manuscript **Received** December 19, 2005;

**Revised** May 1, 2006)

$\mathfrak{S}_i$  : Fermi-Dirac integral of order  $j$

$h$  : Planck constant ( $=6.6262 \times 10^{-34}$ ), J s

$I$  : Laser intensity,  $W/m^2$

$J$  : Laser fluence,  $mJ/cm^2$

$k_B$  : Boltzmann constant ( $=1.38066 \times 10^{-23}$ ), J/K

$L$  : Thickness of a film, m

$N_C$ : Electron-hole pair (carrier) number density,  $1/m^3$

$R$  : Reflectivity

- $t$  : Time, s
- $t_p$  : Pulse duration time (full-width at half maximum), s
- $T$  : Temperature, K
- $U$  : Internal energy, J/m<sup>3</sup>
- $y$  : Spatial coordinate, m
- $\alpha_1$  : One photon band-to-band absorption coefficient, 1/m
- $\delta$  : The impact ionization rate, 1/s
- $\gamma$  : Auger recombination coefficient, m<sup>6</sup>/s
- $\kappa$  : Thermal conductivity, W/m K
- $\lambda$  : Wavelength, m
- $\eta$  : Reduced Fermi level
- $\nu$  : Photon frequency, 1/s
- $\tau$  : Energy relaxation times, s

**Subscripts**

- $A$  : Acoustic phonons
- $C$  : Carriers
- $O$  : Longitudinal optical (LO) phonons.

**1. Introduction**

The ultrashort pulse lasers being of pulses shorter than 10 ps can generate easily very high optical peak power which is enough for full ionization of almost any solid matter (Tien et al., 1998 ; Phinney and Tien, 1998). Non-equilibrium and non-thermal characteristics have opened new

and exciting possibilities in microfabrications, cellular nanobiosurgery technology, measurement and microscopy, environmental technology, and so on (Chlipala et al., 1989). As direct-band-gap materials, in particular, III-V semiconductors have received a tremendous amount of interest from both the microelectronics industry and academia in the last decade since the realization of the promising applications in high-speed electronic devices, optoelectronics, and next-generation display technology. The abundant applications need a better understanding of the energy transport phenomena during fast laser heating.

In fact, the energy transport mechanism during laser irradiation can be explained by electron-hole excitation, photon-carrier-phonon interactions, and recombination processes, as seen in Fig. 1 (Lee, 2005). First of all, a valence electron excited by absorbing the photons results in an electron in the conduction band and a hole in the valence band. The electron-hole pairs (hereafter called carriers) in semiconductors transfer their energies eventually into two different types of phonons being of optical and acoustic modes in the lattice. Here, the term “lattice” in crystallography means a mathematical abstraction of periodic points in space. Basically, a phonon means the discrete value or quantum of vibrational energy due to the particle-wave duality. Since the chem-

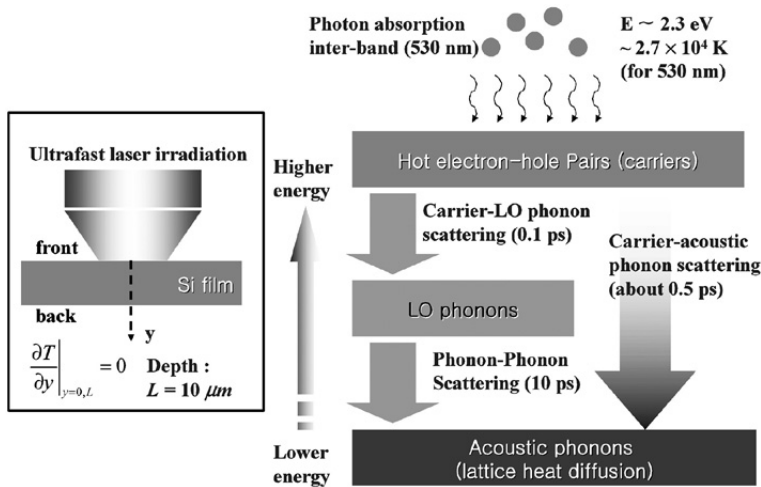


**Fig. 1** Schematics of computational domain and mutual interactions among photons, LO phonons, and acoustic phonons (Lee, 2005)

ical bonds between atoms in a solid are not rigid but act like springs, such vibrations are responsible for energy transport in many solids, and their modes can be either in-phase or out of phase, representing the acoustic branch and the optical branch, respectively (Chen, 2004; Tien et al., 1998). Because the energy level of optical phonons is higher than that of acoustic phonons, they can interact with electromagnetic waves more easily. It is clear that the group velocity of the optical branch is close to zero or negligible compared to that of the acoustic branch. Intrinsically, the optical phonons are associated with an oscillating dipole that scatters radiation, and they scatter and emit acoustic phonons, which are responsible for lattice heat conduction. Moreover, the optical branch influences some of the optical properties of a crystal in real phenomena. At this moment, it should be noted that the recombination process depends substantially on band structures and it becomes very crucial in energy transport mechanism. The recombination process indicates the carrier loss owing to the process in which the free electrons are captured by ionized donors and lose their energy in the nonradiative and radiative ways (Pierret, 1983). In direct-band-gap materials such as GaAs, GaSb, and InAs, three recombination mechanisms are involved (Agrawal and Dutta, 1993): (1) Radiative recombination in which the excited electron and hole recombine and emit a photon, (2) Shockley-Read-Hall (SRH) non-radiative recombination or thermal recombination via the recombination center, in which the electron and the hole recombine and release a phonon to lattice, and (3) Auger recombination, where the extra energy released by the electron and hole recombination will be absorbed by another nearby electron or hole. There have been a number of studies reported that resort mainly to hydrodynamic equations to model electron and phonon transport in practical engineering use (Qiu and Tien, 1994; Lee et al., 2003). However, most of these works did not examine close interactions between longitudinal optical (LO) phonons and acoustic phonons, and they were based on the assumption that the lattice is a single thermodynamic system. This assumption is not valid

generally because there is clearly nonequilibrium energy transport process between two phonons during very short but finite time scale. The efficient way has been introduced to represent the primary path of energy transport by first scattering between carriers and LO phonons and then LO phonons to the acoustic phonons (Tien et al., 1998). Because this approach deals with three different temperatures of carriers, LO phonons, and acoustic phonons, it can be hereafter referred to as the three-temperature model. Of course, this model has been taken in studying thermal nonequilibrium in submicron silicon MOSFETs and GaAs MESFETs (Majumdar et al., 1995a; 1995b). However, there are insufficient works that use the three-temperature model for simulating laser-solid interactions. To date, Lee (2005) investigated the heat transfer characteristics in silicon microstructures irradiated by ultrafast pulse lasers.

By using the three temperature model, the present study thus conducts the extensive simulation for estimation of time and spatial temperature distributions of carriers, LO phonons, and acoustic phonons to investigate their interactions and energy transports in direct bandgap energy materials during subpicosecond pulse laser irradiation. In particular, the role of recombination process on energy transport mechanism is discussed in detail and the influence of laser fluences and pulse widths on nonequilibrium heat transfer are examined.

## 2. Governing Equations and Computational Details

The consistent numerical model should be derived to describe the nonequilibrium between carriers and two different types of phonon. The carrier number density is determined from the conservation equation as follows :

$$\frac{\partial N_c}{\partial t} = \frac{\alpha_1 I}{h\nu} - RR(N_c) + \delta(T_c) N_c \quad (1)$$

$$I = \frac{0.939J(1-R)}{t_p} \exp\left(-\int_0^y \alpha_1 dz\right) \exp\left(-\frac{2.773t^2}{t_p^2}\right) \quad (2)$$

In Eq. (1), the first term on the right-hand side

represents the absorption source term that corresponds to direct transition that excites an electron to the conduction band and creates an electron-hole pair. The final term indicates the carrier generation rate owing to impact ionization process. The second term means the recombination process associated with heating and destruction processes in carrier number density. Unlike indirect-band-gap materials such as Ge and Si, direct-band-gap material such as GaAs, there are three well-known recombination mechanisms (Agrawal and Dutta, 1993).

$$RR(N_c) = \gamma_{sr}N_c + (\gamma_{rad} + \gamma_{SRH})N_c^2 + \gamma_{auger}N_c^3 \quad (3)$$

where  $\gamma_{sr}$ ,  $\gamma_{rad}$ ,  $\gamma_{SRH}$ , and  $\gamma_{auger}$  denote the empirical coefficients via surface recombination, radiative recombination, SRH recombination, and Auger recombination, respectively. For GaAs, at room temperature, the Auger process is not the dominant recombination mechanism even when high concentrations of electrons and holes, whereas radiative recombination dominates in the bulk and surface recombination velocities tend to be quite high. Since radiation recombination does not contribute directly to heating, surface recombination becomes important in heating materials even at room temperature. Since the present study deals with rapid heating process by ultrafast pulsed lasers, however, the surface recombination process is ignored in the present calculation. Since the size of laser beam is large compared to the laser penetration depth, in addition, the short-pulse laser heating of materials can be modeled as one-dimensional. As indicated by Tien et al. (1998) and Lee (2005), in most of previous work the lattice has been assumed to be a single thermodynamic system. Because the time scales for carrier-optical phonon (typically 100 fs) and phonon-phonon (10 ps) interactions are different by two orders of magnitude, however, this assumption cannot be justified. That is why the present study uses the three-temperature model for GaAs microstructures. The energy conservation equations for carriers, LO phonons, and acoustic phonons can be expressed as separately (Tien et al., 1998):

$$\frac{\partial U_c}{\partial t} = \frac{\partial}{\partial y} \left( \kappa_c \frac{\partial T_c}{\partial y} \right) - \frac{3N_c k_B}{2} \left( \frac{T_c - T_o}{\tau_{c-o}} \right) - \frac{3N_c k_B}{2} \left( \frac{T_c - T_A}{\tau_{c-A}} \right) + \alpha_1 I \quad (4)$$

$$\frac{\partial U_o}{\partial t} = \frac{3N_c k_B}{2} \left( \frac{T_c - T_o}{\tau_{c-o}} \right) - C_o \left( \frac{T_o - T_A}{\tau_{o-A}} \right) \quad (5)$$

$$\frac{\partial U_A}{\partial t} = \frac{\partial}{\partial y} \left( \kappa_A \frac{\partial T_A}{\partial y} \right) + \frac{3N_c k_B}{2} \left( \frac{T_c - T_A}{\tau_{c-A}} \right) + C_o \left( \frac{T_o - T_A}{\tau_{o-A}} \right) \quad (6)$$

where,  $U_o = C_o T_o$ ,  $U_A = C_A T_A$ , and  $U_c = C_c T_c + N_c E_g$  where  $E_g$  is the bandgap energy of material. In addition, the relaxation time scales for energy transfer such as  $\tau_{c-o}$ ,  $\tau_{c-A}$ , and  $\tau_{o-A}$  can be rigorously expressed in terms of temperature, frequency, and other factors. Since accurate estimation of these relaxation times is very complicated, those relaxation times are assumed to be constant values from the literature in the present study for simplicity of calculation. For instance, the energy relaxation time between carriers and LO phonons,  $\tau_{c-o}$ , is equal to 0.1 ps (Collins and Yu, 1984). While the relaxation time between the LO phonons and the acoustic phonons,  $\tau_{o-A}$ , is reported to have a rather wide range (Lugli et al., 1989), the present study chooses 10 ps for the calculation. Since optical phonons have negligible group velocity and cannot contribute to lattice heat conduction, on the other hand, there is no heat diffusion term in the right-hand side of Eq. (5). The optical phonons scatter and emit acoustic phonons, which are responsible for the lattice heat conduction, as indicated previously. The important role of optical phonons is to provide the efficient intermediate path for heat transfer from energy source due to photon absorption to energy sink (acoustic phonons). This energy cascade depends highly on relaxation times as well as heat capacities of carriers, LO phonons, and acoustic phonons. The physical properties of GaAs taken from open literature (Tien et al., 1998; Pierret, 1983; Agrawal and Dutta, 1993; Kittel, 1986; Meyer et al., 1980) are listed in Table 1. The recombination rates for different processes are taken from the literature (Kittel, 1986; Seeger, 1991).

**Table 1** Physical properties of a GaAs layer

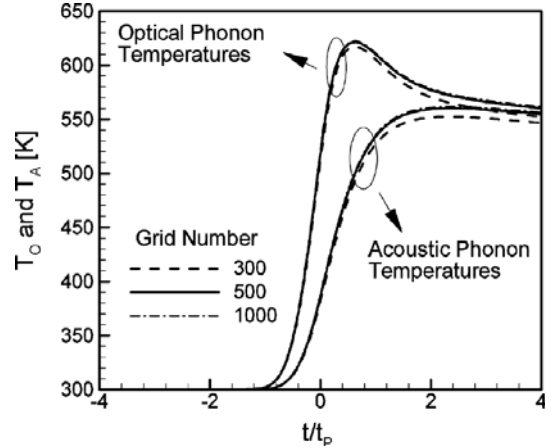
Properties	Expressions
$C_c$	$3N_c k_B$
$C_A$	$9.17 \times 10^5 - 4.40 \times 10^4 (\theta_D / T_A)^{1.948}$ , where $\theta_D \approx 344$ K for GaAs (Kittel, 1986 ; Majumdar et al., 1995b)
$C_o$	$6.86 \times 10^{28} k_B \left( \frac{\theta_E}{T_o} \right)^2 \frac{\exp(\theta_E / T_o)}{[\exp(\theta_E / T_o) - 1]^2}$ where $\theta_E = h\nu / K_B \approx 429$ K for GaAs, (Kittel, 1986 ; Majumdar et al., 1995b)
$k_c$	$k_B^2 \sigma_c \frac{T_c}{q^2} \left[ 6F_2(\eta_c) F_0(\eta_c) - \frac{4F_1^2(\eta_c)}{F_0^2(\eta_c)} \right]$ (Pierret, 1983)
$k_A$	$5.44 \times 10^4 / T_A^2$ (Meyer et al., 1980)
$\tau$	$\tau_{c-A} \approx 0.5$ ps (Majumdar et al., 1995b) $\tau_{c-o} \approx 0.1$ ps (Collins and Yu, 1984) $\tau_{o-A} \approx 10$ ps (Ferry, 1991 ; von der Linde et al., 1980)
R	0.3~0.33 (Meyer et al., 1980)
$E_g$	$1.519 - \frac{5.405 \times 10^{-4} T_A^2}{T_A + 204}$ (Agrawal and Dutta, 1993)

The radiative recombination coefficient of GaAs is expressed as

$$\gamma_{rad}(T_A) = 7.21 \times 10^{-16} \times (E_g(T_A) / E_{gref})^2 \left( \frac{T_A}{300} \right)^{-3/2} \quad (7)$$

In addition, the empirical coefficients for SRH recombination and Auger recombination for GaAs are taken  $10^{-14}$  m<sup>3</sup>/s and  $10^{-43}$  m<sup>6</sup>/s, respectively (Seeger, 1991).

The finite difference method with the fully implicit scheme was used for discretizing the set of governing equations. The initial time was set to  $t_{mit} = -5t_p$  for all cases. Initially, the carrier and the lattice temperatures are maintained at 300 K, and the number density is  $10^{18}$  m<sup>-3</sup> (Pierret, 1983). As seen in Fig. 1, the von Neumann boundary conditions using the zero gradient at  $y=0$  and  $y=L$  are used in this work for temperatures of carrier and two phonons on the basis of the assumption that during the short period of laser heating, heat losses from the front and back surfaces of the GaAs film may be negligible (Lee et

**Fig. 2** Grid independence test

al., 2003). The final solutions are obtained when the relative deviation of each temperature is less than  $10^{-4}$  and the residuals from energy equations are less than  $10^{-4}$  likewise. For 530 nm radiation, all simulations are performed for film thickness  $L = 10$   $\mu$ m. The present work examines the sensitivities of time step and mesh size on the final solutions. For instance, as seen in Fig. 2, the grid number of 500 (uniform grids), which corresponds 20 nm, is used in all calculations through grid-independent tests.

### 3. Results and Discussion

For various laser fluences at a fixed pulse, i.e., 10 ps, Fig. 3 illustrates in-situ estimations of carrier temperatures and two different phonon temperatures at the film surface with respect to time normalized by the pulse duration. As one might expect, the carrier temperature increases rapidly compared to the temperatures of LO phonons and acoustic phonons. The nonequilibrium takes place due to the difference between energy relaxation times and laser pulse durations. Under nonequilibrium state, the carriers do not lose their energy to the lattice phonons within a certain time period, remain quite energetic, and approach their maximum values. It is interesting to note an existence of two-peak structure in the carrier temperature. The second peak increases with laser fluence, whereas the first peak is inde-

pendent of laser fluence. The first peak occurs in the early stage of laser exposure because carrier heat capacity is several orders of magnitude smaller than phonon heat capacities (regime 1). Meanwhile, the presence of second peak is clearly because of non-radiative recombination process that heats the plasma (regime 2). In Fig. 3(b) showing time evolution of LO and acoustic phonon temperatures, the nonequilibrium between two phonons is observed during the finite time, and its extent increases with laser fluence. This confirms that the assumption of single thermodynamic system is no longer valid for ultra-short

pulse laser heating problems. This nonequilibrium would be mainly because of the difference of scattering times between two different phonons.

Figure 4 shows the influence of pulse duration on three different temperatures when  $J=10\text{ mJ/cm}^2$ . In the regime 1, the transient behavior of carrier depends on pulse duration because under same laser fluence, laser energy deposited on materials is more intense as pulse width decreases. Hence, the peak value of carrier temperature increases with decreasing laser pulse duration. It is noted that for  $t_p=100\text{ ps}$ , two phonon temperatures are nearly in equilibrium state as seen in

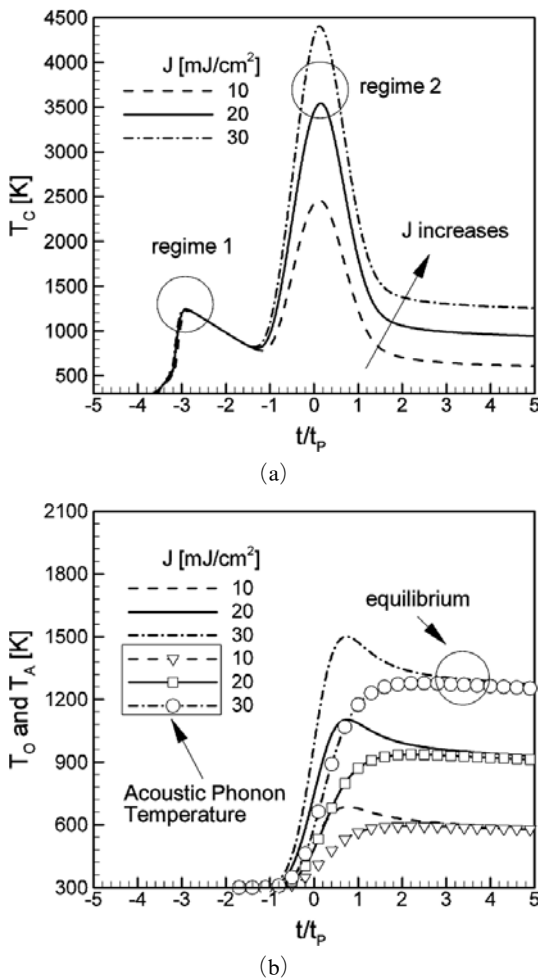


**Fig. 3** The temporal distributions of (a) carrier temperatures and (b) two different phonon temperatures for different laser fluences at  $t_p=10\text{ ps}$

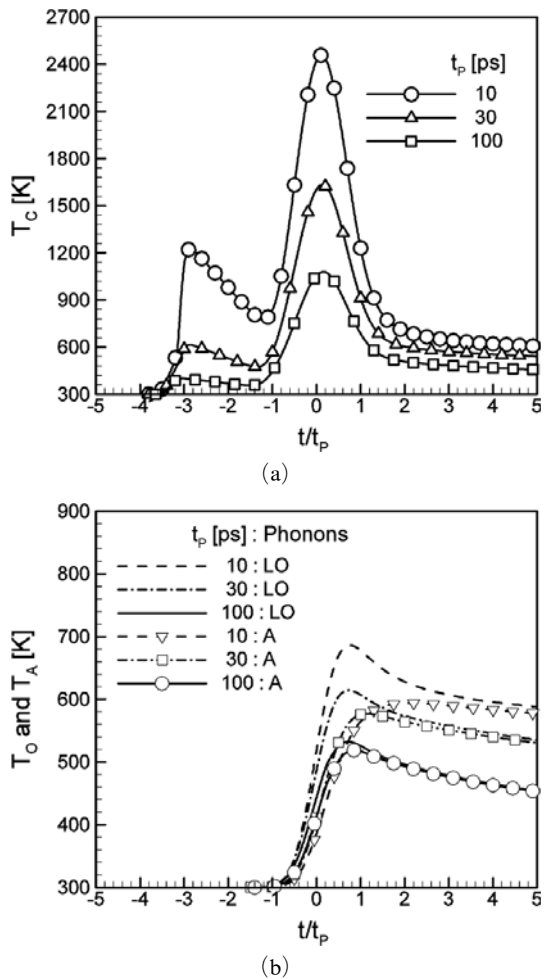


**Fig. 4** The temporal distributions of (a) carrier temperatures and (b) two different phonon temperatures for various laser pulses at  $J=10\text{ mJ/cm}^2$

Fig. 4(b) because of pulse duration much longer than relaxation times. In this case, thermal equilibrium assumption would be reasonable. However, for subpicosecond pulse lasers, nonequilibrium between two phonons should be considered. It is thus found from the results that the energy transport in GaAs film structure irradiated by picosecond pulse lasers is achieved by the following mechanism: At the early stage of laser exposure, the carrier energy first increases substantially because the carrier heat capacity is smaller than those of two phonons. After the finite time period, they lose their energy to phonons through emitting LO and acoustic phonons, and nonequilibrium causes energy transport, consequently. As seen in Fig. 4(b), the time when LO phonon temperature starts to increase is slightly faster than that when acoustic phonon does. This time lag is not only because the specific heat of LO phonons is a bit smaller than that of acoustic phonons as indicated by Lee (2005), but because there is the finite relaxation time between two phonons as shown in Table I. For longer pulse durations, the time lag is not observed because of thermal equilibrium state between two phonons. In addition, at very short time duration, the energy transport from carriers to LO phonons is dominant in causing nonequilibrium. It leads to the rapid increase in LO phonon temperatures. In GaAs or other III-V materials, even stronger coupling to electron-hole pairs is present due to the polar interactions and it makes LO phonons emitted more efficiently. Since optical phonon energies are higher than those of acoustic phonons, optical phonon emission is a faster and more efficient way to transfer energy. Figure 5 represents the spatial temperature distributions of LO and acoustic phonons at  $t=0$  ps when laser energy peaks. The maximum diffusion depth is estimated about  $0.5 \mu\text{m}$  when all temperatures are in equilibrium. It is clearly observed that as laser pulse increases, temperature difference between two phonons decreases. It means that two phonons are in equilibrium state.

As indicated previously, the recombination process that takes place is very important in energy transport in GaAs materials. To inves-

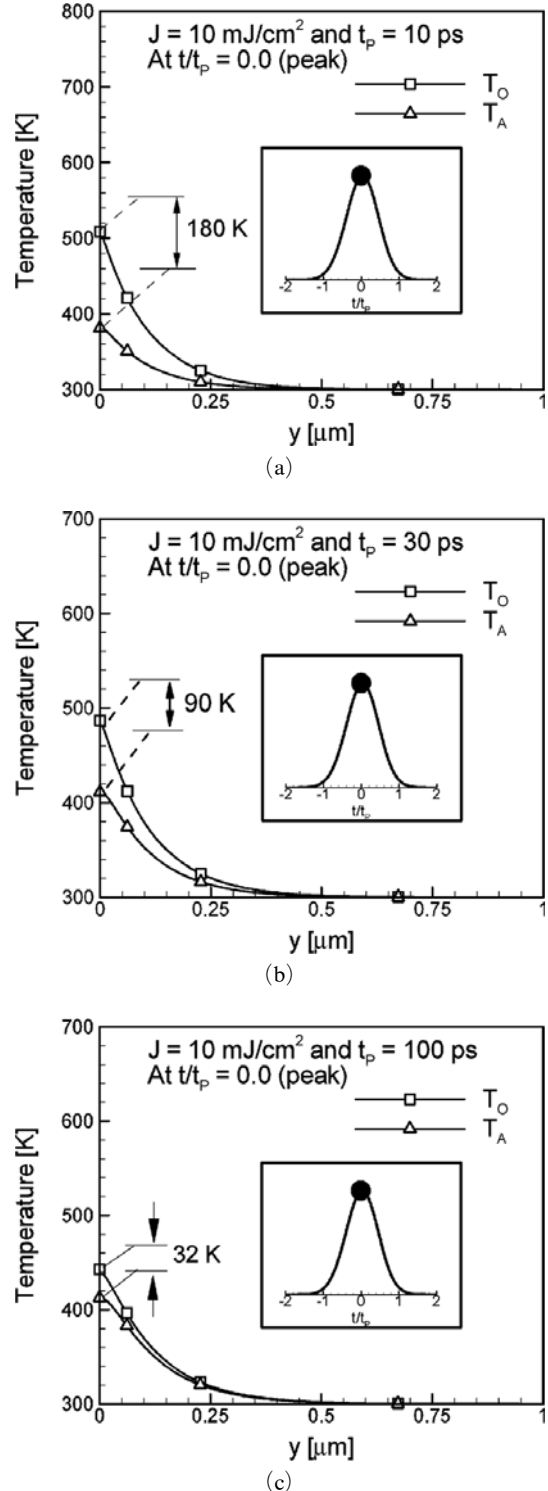


Fig. 5 The spatial distributions of LO and acoustic phonon temperatures for various pulse widths at  $t=0$  when laser energy peaks

investigate the influence of recombination, it is necessary to examine the role of recombination process on carrier number density. Three different processes such as radiative recombination, SRH recombination, and Auger recombination are investigated in the present study under same irradiation conditions, i.e.,  $J=10 \text{ mJ/cm}^2$  and  $t_p=10 \text{ ps}$ . For doing this, this study deals with four cases: In case 1, all recombination processes are included. In case 2, Auger recombination process is only considered. In case 3, two processes such as Auger and SRH recombination are only involved. In case 4, Auger and radiative recombination processes are used for calculation. As seen in Fig. 6(a), cases 1 and 3 show similar tendency but cases 2 and 4 represent quite different patterns in regime 2 where recombination effects are dominant as discussed previously. Here, what cases 2 and 4 predict lower carrier temperatures near the region 2 is because the extent of reduction in carrier number density via recombination process is underpredicted. In regime 2, the carrier temperature again rises near  $t=0$ , at which the number density increases and recombination process converts carrier ionization energy into kinetic energy at a sufficiently large rate to again cause the carrier temperature to increase (Driel, 1987). This means that the energy released by the recombination is transferred to the surviving carriers. Although the carrier temperature falls again once the carrier number density begins to decrease, there remains a significant difference between carrier and lattice temperatures for long times relatively due to on-going recombination processes. Therefore, the SRH recombination, one of non-radiative recombination processes, plays an important role in decreasing carrier number density. According to previous works (Lee et al., 2003; Pierret, 1983), Auger recombination is activated more vigorously when the carrier number density is very high, whereas the SRH recombination rate in GaAs event at room temperature is quite high compared to Auger recombination rate. Meyer et al. (1980) suggested that as temperature increases, Auger recombination becomes dominant as in the other materials. However, their suggestion is perhaps not valid for ultrafast laser heating in

GaAs materials. Figure 7 represents various recombination rates during laser irradiation and it can support some results discussed previously. In fact, it turns out that SRH recombination rates have already increased considerably, compared to those of other processes at the initial stage of laser irradiation. It is true that Auger recombination becomes an important process when carrier number density is very high (Pierret, 1983). When carrier number density is reduced due to SRH recombination initially, however, Auger recombination process becomes minor process. Besides, even radiative recombination rate is higher than Auger recombination rate. It is thus found that SRH recombination is the dominant process which

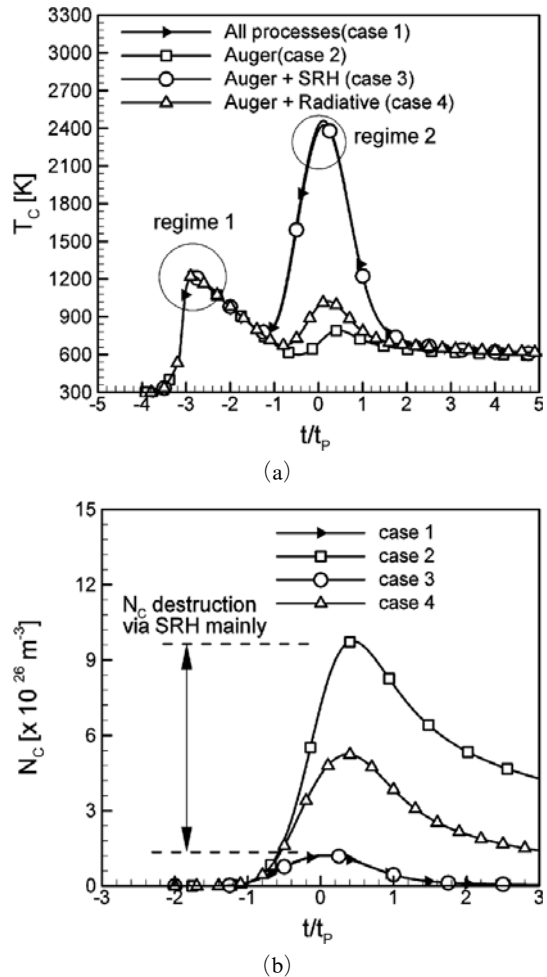


Fig. 6 The time evolution of carrier temperature and carrier number density for different cases



should be considered for dealing with the direct bandgap materials, whereas Auger recombination can be neglected even at high temperature. This result is very consistent with that of Zhang et al. (2002). Furthermore, Fig. 8 depicts the spatial distribution of various recombination rates. As  $y$  increases, the difference among recombination rates increases. Thus, it is concluded that Auger recombination is obviously negligible compared to two other recombination processes. Those facts confirms that the presence of second peak as found in Figs. 3 and 4 is mainly caused by the SRH recombination process.

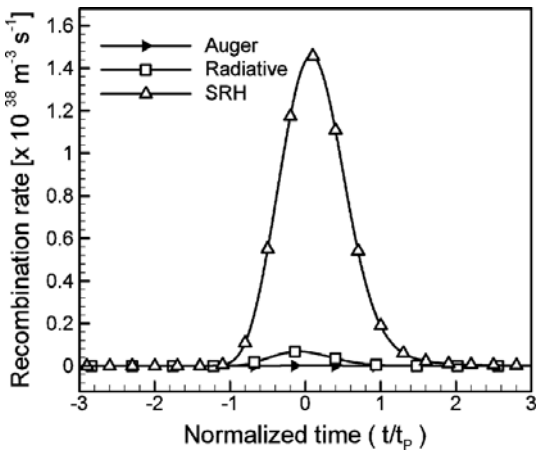


Fig. 7 The temporal behaviors for each of recombination rates

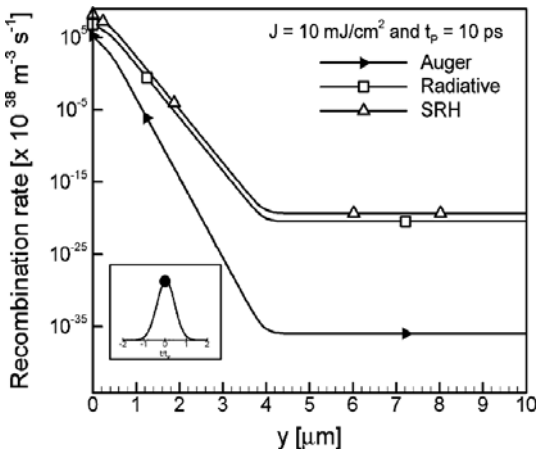


Fig. 8 The spatial distribution of recombination rates for or each of recombination rates

### 4. Conclusions

The present study reports numerically the micro-scale heat transfer characteristics in GaAs thin film irradiated by picosecond pulse lasers. The three temperature model for GaAs is presented to examine the interactions among photons, carriers, LO phonons, and acoustic phonons. This article also discusses the influence of pulse duration and laser fluence on heat transfer as well as the role of recombination on the variation of carrier number density. The following conclusions can be drawn. First, the nonequilibrium among carriers, LO phonons, and acoustic phonons is present during a finite time after which all of them are gradually equilibrated as time goes. A two-peak structure in carrier temperature can be found, and it occurs due to recombination as well as difference of heat capacities. Second, it turns out that the three-temperature model used is appropriate because LO phonons and acoustic phonons are in nonequilibrium state within such lagging times. For longer pulses, this lagging effect eventually disappears. Finally, at the initial stage of laser irradiation, SRH recombination rates have already increased sufficiently, compared to those of other processes. This is because initially abrupt increase in carrier number density no longer permits Auger recombination to be activated. Furthermore, it is found that Auger recombination can be neglected even at high temperature for ultrafast laser heating problem in GaAs thin film structures.

### Acknowledgments

The authors gratefully acknowledge financial support from the Micro Thermal System Research Center sponsored by the Korea Science and Engineering Foundation.

### References

Agrawal, G. P. and Dutta, N. K., 1993, *Semiconductor Lasers*, Wan Nostrand Reinhold, NY.  
 Chen, G., 2004, *Nanoscale Energy Transport*

and Conversion : A Parallel Treatment of Electrons, Molecules, Phonons, and Photons, Oxford University Press.

Chlipala, J. D., Scarforne, L. M. and Lu, C. Y., 1989, "Computer-Simulated Explosion of Poly-Silicide Links in Laser-Programmable Redundancy for VLSI Memory Repair," *IEEE Transaction of Electronic Devices*, Vol. 36, pp. 2433~2439.

Collins, C. L. and Yu, P. Y., 1984, "Generation of Nonequilibrium Optical Phonons in GaAs and Their Application in Studying Intervalley Electron-Phonon Scattering," *Physical Review B.*, Vol. 30, pp. 4501~4515.

Ferry, D. K., 1991, *Semiconductors*, Macmillan, New York.

Kittel, C., 1986, *Introduction to Solid State Physics*, 6<sup>th</sup> edition, Wiley, New York.

Lee, S. H., 2005, "Nonequilibrium Heat Transfer Characteristics During Ultrafast Pulse Laser Heating of a Silicon Microstructure," *Journal of Mechanical Science and Technology*, Vol. 19, No. 6, pp. 1427~1438.

Lee, S. H., Lee, J. S., Park, S. and Choi, Y. K., 2003, "Numerical Analysis on Heat Transfer Characteristics of a Silicon Film Irradiated by Pico-to-Femtosecond Pulse Lasers," *Numerical Heat Transfer, Part A*, Vol. 44, No. 8, pp. 833~850.

Lugli, P., Bordone, P., Reggiani, L., Rieger, M., Koccar, P. and Goodnick, S. M., 1989, "Monte Carlo Studies of Nonequilibrium Phonon Effects in Polar Semiconductors and Quantum Wells, 1. Laser Photoexcitation," *Physical Review Letters*, Vol. 39, pp. 7852~7865.

Majumdar, A., Fushinobu, K. and Hijikata, K., 1995a, "Effect of Gate Voltage on Hot-Electron and Hot-Phonon Interaction and Transport in a Sub-Micron Transistor," *Journal of Applied*

*Physics*, Vol. 77, pp. 6686~6694.

Majumdar, A., Fushinobu, K. and Hijikata, K., 1995b, "Heat Generation and Transport in Sub-micron Semiconductor Devices," *ASME Journal of Heat Transfer*, Vol. 117, pp. 25~31.

Meyer, J. R., Kruer, M. R. and Bartoli, F. J., 1980, "Optical Heating in Semiconductors : Laser Damage in Ge, Si, InSb and GaAs," *Journal of Applied Physics*, Vol. 51, pp. 5513~5522.

Phinney, L. M. and Tien, C. L., 1998, "Electronic Desorption of Surface Species Using Short Pulse Lasers," *ASME Journal of Heat Transfer*, Vol. 120, pp. 765~771.

Pierret, R. F., 1983, *Advanced Semiconductor Fundamentals, Modular Series on Solid State Device*, Vol. 6, Addison-Wesley Publishing Company.

Qiu, T. Q. and Tien, C. L., 1994, "Femtosecond Laser Heating of Multi-Layer Metals — I. Analysis," *International Journal of Heat and Mass Transfer*, Vol. 37, pp. 2789~2797.

Seeger, K., 1991, *Semiconductor Physics : An Introduction*, 5<sup>th</sup> edition, Springer, New York.

Tien, C. L., Majumdar, A. and Gerner, F. M., 1998, *Micro-scale Energy Transport*, Taylor & Francis, Washington D.C..

van Driel, H. M., 1987, "Kinetics of High-Density Plasmas Generated in Si by 1.06- and 0.53- $\mu\text{m}$  Picosecond Laser Pulses," *Physical Review B.*, Vol. 35, No. 15, pp. 8166~8176.

Von der Linde, D., Kuhl, J. and Klingenburg, H., 1980, "Raman Scattering from Nonequilibrium LO Phonons with Picosecond Resolution," *Physical Review Letters*, Vol. 44, pp. 1505~1508.

Zhang, X., Wen, J. and Sun, C., 2002, "Thermal and Carrier Transport Originating from Photon Recycling and Non-radiative Recombination in Laser Micromachining of GaAs Thin Films," *Applied Physics A*.